Magnetic Pulse Crimping of Power Cables: Process Simulation & Performance Characterization

J.-P. Cuq-Lelandais[1*], N. Innocenti[2], W. Gage[2], C. Huteau[1], G. Daulhac[1] and N. Mrozowski[1]

[1] I-Cube Research / Bmax SAS – 30 boulevard de Thibaud - ZI Thibaud - BP 90423 - 31 104 Toulouse CDX 1 – France
[2] Bmax USA - 2870 Technology Drive - Rochester Hills, MI 48309 USA
*Corresponding author. Email : jean-paul.cuq@icube-research.com

Abstract

Magnetic Pulse Crimping (MPC) represents an interesting alternative to mechanical crimping. This solution is a contactless process using dynamic Lorentz forces induced by high pulse power electrical discharge through a coil. MPC has proven to be effective for cables terminals with both high electrical and mechanical performances. This solution differs from conventional methods for cables with large cross-sections for high voltages especially those manufactured for electric vehicles. The challenge lies in the high thickness of the terminal and the cable to be crimped together while maintaining the performance of the connection during use and ageing, that can be hard to hold with traditional processes. The aim of this work is to characterize the electrical resistance of 120 mm² power cables terminals that are assembled by MPC, with the goal of reducing the process width and potentially reduce the lug mass. First, a numerical study of the process is performed in order to design and characterize the crimping level depending on main process parameters, in particular through the compaction level of the assembly. Then, an experimental study has been carried out by testing assemblies with different crimping widths and generator energies, in order to reduce the crimped length without degrading the performance and repeatability. For each case, the electrical resistance of the cable/lug interface is measured, before and after exposure to thermal and humidity cycling representative of real-life conditions. The results are compared with samples produced using mechanical crimping to compare the performances and repeatability of each process respectively.

Keywords

High Pulse Power (HPP), Magnetic Pulse Crimping (MPC), Power Cable, Multiphysics Simulation

1 Introduction & Stakes

Magnetic Pulse Crimping (MPC) offers a promising alternative to traditional mechanical crimping. It is a contactless process that utilizes dynamic Lorentz forces generated by a high-power electrical pulse passing through an inductor. MPC has demonstrated its effectiveness for cable terminals, delivering both excellent electrical and mechanical performance (M. Kim and J. Shim, 2023). Unlike conventional techniques, MPC is particularly well-suited for cables with large cross-sections intended for high-voltage applications (N. Ali, et al., 2023), such as those used in e-mobility—typically up to 200 mm².

The main challenge lies in the significant thickness of both the terminal and the cable, which can pose problems for traditional processes such as mechanical crimping. The pressure required to properly crimp the terminal in a quasi-static process must compress all strands uniformly across the cross-section. This generates considerable internal stresses within the cable and often requires a relatively bulky connector to maintain a reliable hold. However, current industry trends aim to reduce product weight and optimize manufacturing costs, which positions MPC as a strong candidate for such applications.

The purpose of this project is to demonstrate that MPC offers equivalent—or even superior—performance and repeatability compared to mechanical crimping, and to show that it is possible to optimize the process parameters to produce shorter crimped assemblies, thereby reducing overall assembly weight. Both numerical and experimental investigations were conducted by testing three MPC configurations, with crimping width and generator energy levels as the main varying parameters. Electrical resistance at the cable/lug interface was measured before and after subjecting the samples to thermal and humidity cycling. The performance of these samples was then compared to that of assemblies produced using mechanical crimping.

2 MPC Power Cables Simulation & Design

The study case selected for this works is a classical copper lug/cable terminal with a 120 mm² section. The main data related to this assembly are summarized in the **Table 1**.

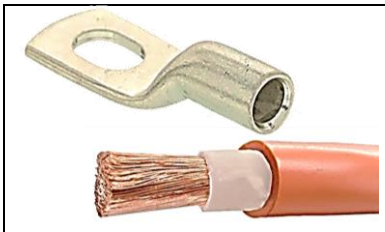

Lug Characteristics		120mm² Conductor cable	
Outer Diameter	21.8 mm	Outer diameter	15.1 mm
Lug Thickness	2.5 mm	Single wire diam.	0.51 mm
Working Length	26 ± 2 mm	Wires number	589
Material	Copper-ETP	Wire material	Copper
Finish	Tin over Nickel	Electrical res.	0.153 mΩ/m

Table 1: *Assembly to be crimped main characteristics*

MPC between two cylindrical pieces is performed by discharging a high current —up to 1MA over 20 µs —with a capacitive bank through a coil (see **Figure 1**). The generator used is designed by Bmax® and can store up to 64 kJ. The pulse induces an eddy current, first in a field shaper, then in the conductive workpiece (copper lug) located inside the

tooling. The produced strong magnetic field creates Lorentz forces accelerating the lug away from the coil (**Figure 2a**). The deformed part then impacts and crushes the cable. As minimum contact resistance is sought for such assemblies, crimping quality strongly depends on two parameters: the compaction level and the lug/strands contact surface.

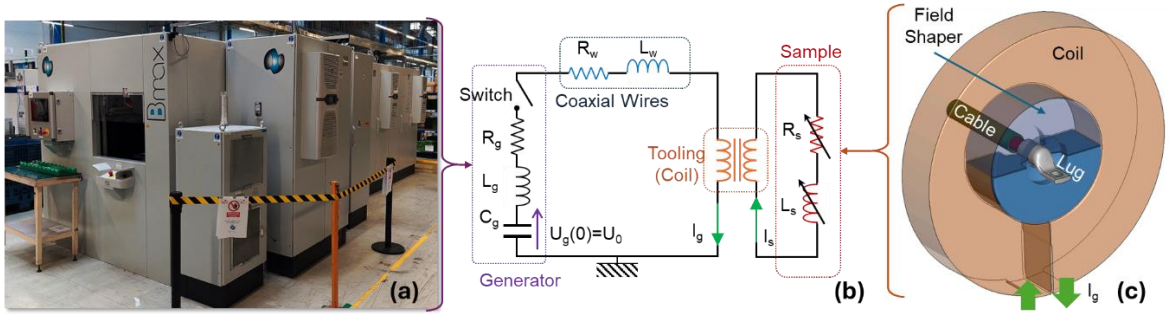

Figure 1: *Magnetic Pulse Crimping setup: Bmax generator and workstation (a) ; Equivalent electrical eircuit (b) ; Process tooling scheme (c)*

The first step of this study is to determine the main process parameters for 120 mm² terminals. An analytical approach can be used to link the generator parameters to the mechanical loading applied on lug. The system can be modelled as a series RLC initially charged at a given energy level E_0. By solving this circuit, the peak current pulse characteristics can be evaluated (**Eqs. 1 to 3**). Then, the magnetic pressure loading is deduced from the electromagnetic relations under a radial 1D assumption (**Eq. 4**) and non-magnetic materials (magnetic permeability $\mu = \mu_0 = 4\pi \cdot 10^{-7}$ H/m). The pressure evolves as a damped square sine wave and its magnitude P_{max} is proportional to the generator energy (**Eq. 5**) and inversely proportional to the square root of the field shaper's active zone (AZ). This non-trivial dependence includes the maximum B-field relation (B_{max}), with a shape factor (k_{sh}) accounting for inductor edge effects (H. Knoepfel, 1970), and also results from the tooling inductance. The latter influences the current/voltage relationship through the k_u coefficient. The coefficient linking the maximum magnetic pressure (P_{max}) to the stored energy can be obtained through dedicated EM 2D-simulations, yielding k_P=1.3 kPa.√m/J.

While the energy required to achieve a given mechanical impulse can be estimated using this approach for a fixed geometrical configuration, the corresponding assembly compaction level is not straightforward to determine. Thus, the next step aims to establish a relationship between the magnetic pressure and the cable's compacted state after the process.

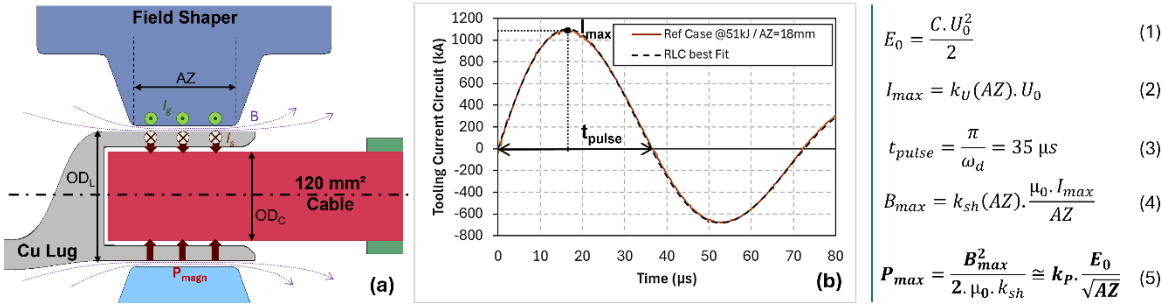

$$E_0 = \frac{C.U_0^2}{2} \quad (1)$$

$$I_{max} = k_U(AZ).U_0 \quad (2)$$

$$t_{pulse} = \frac{\pi}{\omega_d} = 35\ \mu s \quad (3)$$

$$B_{max} = k_{sh}(AZ).\frac{\mu_0.I_{max}}{AZ} \quad (4)$$

$$P_{max} = \frac{B_{max}^2}{2.\mu_0.k_{sh}} \cong k_P.\frac{E_0}{\sqrt{AZ}} \quad (5)$$

Figure 2: *MPC process principle (a), Typical current pulse (b), and Basic equations*

As MPC process occurs in a timescale of tens of microseconds, dynamic time-resolved simulations are useful for analysing the physical phenomena involved in compaction. MPC modelling is performed with LS-DYNA, a 3D parallel Magneto-Hydro-Dynamic (MHD) multiphysics code. The electromagnetic solver employs the eddy current approximation. Maxwell's equations are solved using a Finite Element Method (FEM) for solid conductors, coupled with a Boundary Element Method (BEM) to account for the surrounding air or insulators. To characterize the cable compaction behaviour submitted to a compressive pulse, a 2D mechanical model of the cross-section of the lug and multi-strand cable assembly is developed. The cable is represented by all its individual wires. This model enables visualization of the compaction process, as shown in **Figure 3** (A.K. Rajak and S.D. Kore, 2018R.D. Krieg, 1972). When the pressure pulse is applied to the lug outer diameter, the latter is accelerated and then impacts the outer cable strands. The wires begin to compress, and a compaction wave propagates towards the centre of the cable, where an overpressure is observed. A secondary pressure wave then expands back toward the lug. This effect can generate an undesired bounce-back of the ring, depending on the loading characteristics.

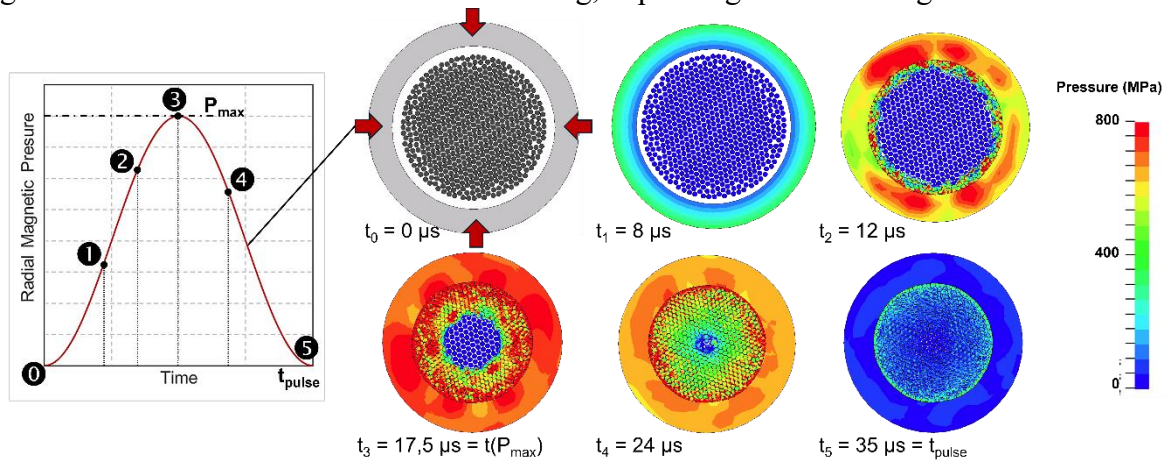

Figure 3: *2D 120mm² Cu cable compaction – P_{max} = 500 MPa & t_{pulse}= 35 µs*

The compaction level evolution is monitored via the cable's volumetric strain. The latter can be linked to the magnetic pressure peak P_{max}, leading to the **Figure 4**. A minimum pressure P_0 = 65 MPa is required to compress the lug to the cable outer diameter. The loading threshold to ensure a full compact cable (i.e. compacted cross-section = 120 mm²) is P_c = 485 MPa. Beyond this limit, the pressure increases exponentially to further compact the cable.

Thanks to this model, one can link directly the generator energy to the compaction level with **Eq. 5**. The experimental campaign to define is based on a reference configuration and two variations. The reference case uses a field shaper with an 18 mm active zone (AZ on **Figure 2)** with an energy leading at full compaction threshold: $P_{max,ref}$ = 500 MPa, equivalent to $E_{0,ref}$ = 51 kJ. The two other cases will employ a narrower field shaper and crimped zone (AZ=12 mm). Case #2 is designed to obtain the same compaction level ($P_{max,\#2}$ = $P_{max,ref}$), leading to an initial energy of $E_{0,\#2}$ = 36 kJ. Conversely, Case #3 has the same energy as the Ref. case, implying a higher loading of $P_{max,\#3}$ = 625 MPa.

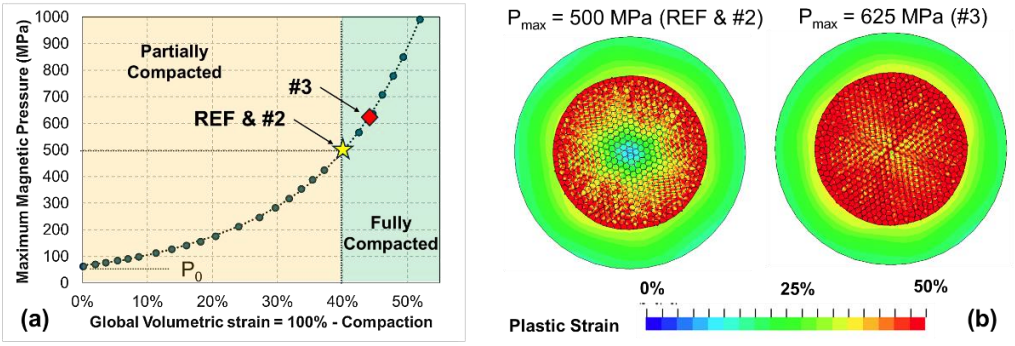

Figure 4: *120mm² Cu cable compaction level in function of the magnetic pressure peak (a) ; 2D Multi-strand final deformations for all the designed cases (b)*

When considering the high number of wires that comprise the cable, this approach is not suitable for a 3D complete process analysis. A good alternative is to model it as a single part with an equivalent transversely isotropic law. The axial component of the model (parallel to the strands axis) is an elastic-plastic bilinear law with a variable bulk modulus depending on the volumetric strain. The transverse behaviour of the material is represented by a compaction model (see **Figure 5a**) similar to those used to model foam and soils (R.D. Krieg, 1972). The compression curve can be identified by measuring some key data in the multi-strand simulations. Several compression steps are visible: from the initial state (O), a zero-plasticity low pressure pre-compaction stage (I) establishes contact between neighbouring strands (II). Then the real compaction is activated, where the strands contact increases and shapes become hexagonal. Total compaction (no porosity) is reached at high pressure (IV). Beyond this limit, the material acts as bulk copper. The compaction law validity can be verified by benchmarking it to the 2D multi-strands simulations, where the cable is replaced by a single disk (see **Figure 5b**). Both methods show a good accordance in terms of compaction level. The equivalent law successfully reproduces the compressive wave and the over-pressure at the cable centre. Moreover, its calculation cost is about ten times lower than the multi-strand model.

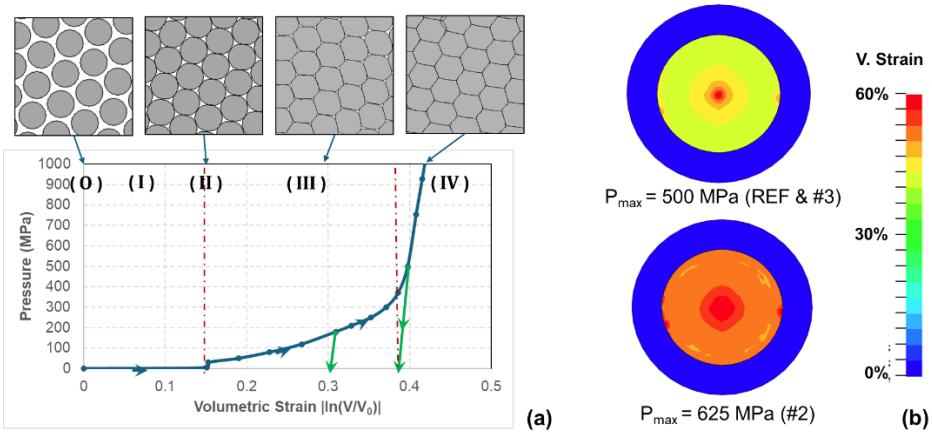

Figure 5: *Transverse pressure compaction law for a 120mm² Cu cable (a); Equivalent compaction for the designed configurations (b)*

3 Experimental Results & Comparison to Modelling

The three configurations determined in §2 were tested experimentally, with 20 samples per case. In addition, traditional mechanical crimping was performed on the same assembly configuration. The MPC samples can serve as a reference database to verify the validity of the simulation model.

A first point of comparison can be established through a measurement of the assembly geometry after the process. 3D scans taken for each configuration (**Figure 6a**) were used to extract the evolution of the terminal cross-sections, shown on **Figure 6b**. Between the reference case and case #2, the minimum compression ratio, obtained at the centre of the active zone, is similar. Case #3 exhibits a higher level of compaction.

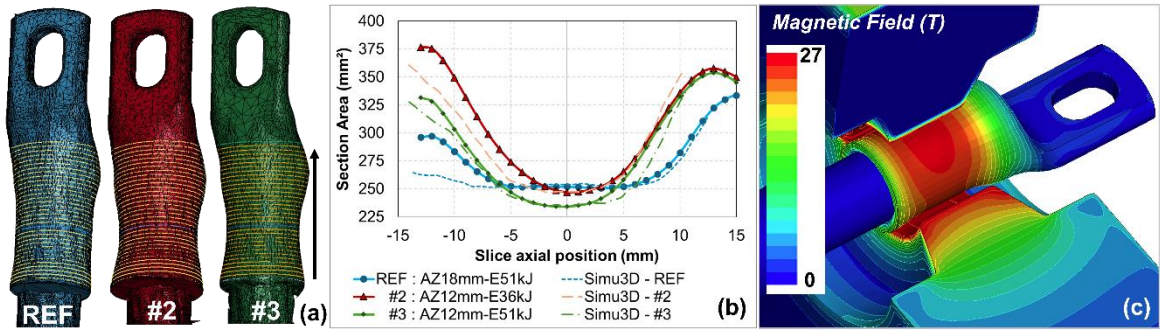

Figure 6: *3D scans of experimental MPC samples (a) – Samples assembly areas and model refits along the cable axis (b) – 3D MPC simulation at peak pressure (t=17.5 µs) for the Reference Case (AZ=18 mm E_0=51 kJ) – colormap = magnetic mield (c)*

3D MHD simulations of the MPC process were carried out for each configuration, using the RLC circuit corresponding to the generator as input. The inductor materials, made of CuCrZr alloy, were modelled using a viscoplastic behaviour law characterised in-house (N. Mrozowski, et al., 2025). The cable is represented by the equivalent law established in §2.3. Numerical profiles show good overall agreement. However, there are discrepancies in geometry, with flatter profiles than those observed experimentally, particularly at the lug tips. This may be attributed to the constitutive behaviour, modelled with a bilinear elastic-plastic law, which may be insufficient to properly reproduce local deformations.

In addition to the 3D scans, observations of the minimum cross-section (slice at position 0 on **Figure 6b**) for each case allow the compaction of the cable to be assessed by measuring the component areas (see **Figure 7**). The reference case and case #2 show similar levels of compaction, while case #3 is more compact, with almost no porosity, reaching a compaction rate of approximately twice that of the reference cross-section (120 mm²). All three configurations are close to the levels predicted by the 2D multi-strand model.

The same analysis was carried out on a mechanically crimped cable with a compaction rate similar to the reference case. In this case, compaction is seen to be inhomogeneous, concentrated mainly in the central region with highly deformed strands, leaving numerous inter-strand voids elsewhere, which may adversely affect joint performance.

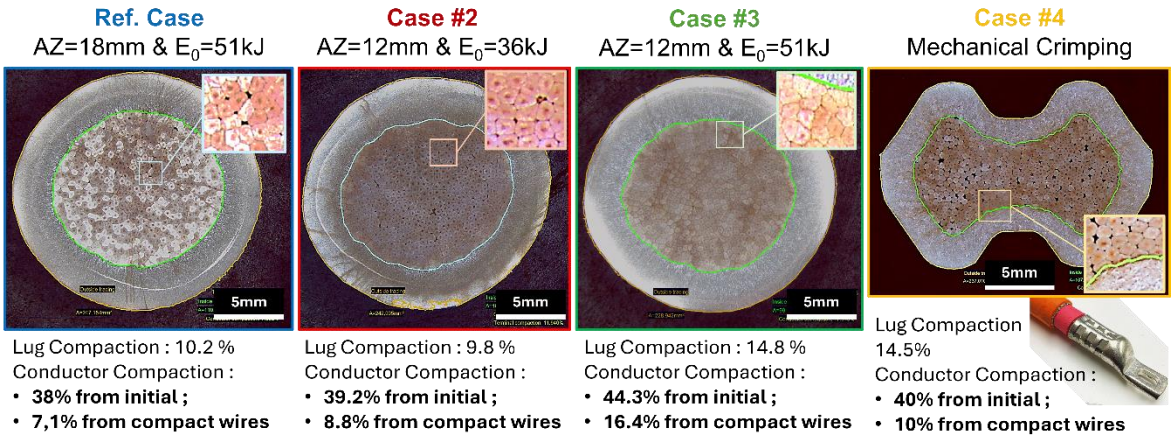

Figure 7: *MPC and mechanical crimping samples optical micrographs at the minimum compacted section*

4 Assemblies' Electrical performances

All crimped cables, 20 per configuration, are then tested to determine the electrical resistance of the interface. Typically, resistances of the order of 10 μΩ or less are sought in order to optimize link heating. Initially, the measurement, presented on the **Figure 8** is carried out for a fresh crimp. Minimal resistances with good repeatability, approx. 5 μΩ, can be observed for the reference case maximizing the contact area, as well as the iso-energy case #3, with less crimped area but more compaction. Case #2, on the other hand, although iso-compacted with the reference case, shows a much higher (12 μΩ) and dispersed resistance. This is probably due to a reduced contact surface compared with the reference case. The same applies to a lesser extent to mechanical crimping (7 μΩ). In this case, the reduced effective contact surface is located in the grooves created by the crimping tool.

Next, the samples are subjected to two cycling tests, commonly used to qualify on-board electrical connections:

1. Purely thermal, with a -40/140 °C amplitude, on a 15 min cycle period, over 500 cycles.
2. Slow thermal cycling in an environment with 95% relative humidity, with a range of 25/55 °C, 10 cycles of 24 hours each.

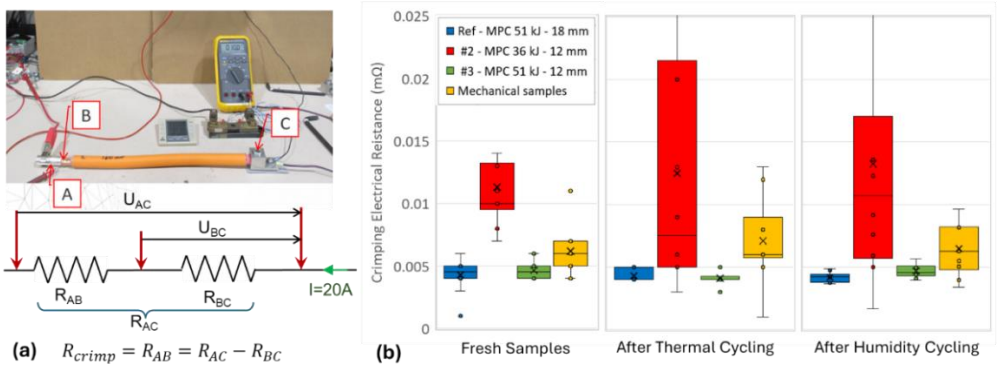

Figure 8: *Interface electrical resistance measurement principle (a); Mechanical and MPC electrical resistance for fresh, and after thermal and humidity cycling (b)*

The assembly resistance is measured after each test. It can be noted that the Reference and Case #3 maintain stable and excellent performance. Similar trends are observed for mechanical crimping, which retains a higher resistance and variability than the best MPC cases. MPC Case #2 resistance is significantly degraded and shows a larger variance after thermal cycling, probably caused by an insufficient contact zone versus compaction ratio. This may lead to contact loosening during thermal cycling, which exaggerates the observed dispersion. Humidity cycling does not affect the results observed. One reason that could explain this lack of variance is that these tests are not demanding enough to produce ageing that would significantly degrade assembly performance. Further investigations are required to verify whether they are sufficiently representative of actual on-board conditions.

5 Conclusions

This study investigated the crimping of power cables used for electric mobility, from both a numerical and experimental point of view. Simulations were used to better understand the MPC process and model the behaviour of a cable made up of a bundle of strands. This led to the identification of an equivalent orthotropic compaction law, which considerably reduces calculation times, making it suitable for 3D analysis. 3D MPC simulations were compared with experimental results with a good accordance overall. The performance of crimped assemblies was also characterized before and after cyclic testing. It was shown it is possible to obtain low-resistance assemblies with a good repeatability. MPC has been compared with mechanical crimping, and shows a good relative resistance decrease in the MPC best cases, by 25% on average. Moreover, it was demonstrated it was possible to reach similar performance at equal energy by reducing the crimped width from 18 to 12 mm and locally increasing the compaction state. This result can serve as basis to move towards optimised compact crimps, that can lightened by 10% in order to reduce their cost. Some future investigations could follow the same direction, by working on the lug thickness.

References

M. Kim and J. Shim, 2023, Selection of Magnetic Pulse Crimping Process Conditions to Improve Crimped Terminal Quality, Metals, 13(11), p1903.

N. Ali, et al., 2023, Experimental investigations on magnetic pulse crimping of copper lug, Engineering Research Express 5 015055

H. Knoepfel, 1970, Pulsed High Magnetic Fields - Physical Effects and Generation Methods Concerning Pulsed Fields Up To the Megaoersted Level. ISBN Elsevier 0444100350

A.K. Rajak and S.D. Kore, 2018, Comparison of different types of coil in Electromagnetic terminal-wire crimping process, J. Manuf. Process. 34, pp. 329–338.

R.D. Krieg, 1972, A Simple Constitutive Description for Cellular Concrete, Sandia National Laboratories, Albuquerque, NM, Report SC-DR-72-0883.

N. Mrozowski, et al., 2025, Determination of the High Strain Rate Behavior of a CuCrZr Alloy Using an Electromagnetic Forming Test Bench, This conference.